πN S_{11} partial-wave amplitude near the ηn production threshold*

Ramesh Bhandari and Yung-An Chao†
Department of Physics, Carnegie-Mellon University, Pittsburgh, Pennsylvania 15213
(Received 16 August 1976; revised manuscript received 28 September 1976)

From an analysis of the $\pi^- p$ backward differential cross-section data, which clearly shows a cusplike structure near the ηn threshold, we deduce, using partial-wave unitarity relations, the size and the orientation of the cusp. The cusp appears because of the strong coupling of the ηn channel to an N' resonance just above its threshold. Using the above information on the cusp, the πN S_{11} partial-wave amplitude is fitted through the ηn threshold and the resonance. The effect of the size of the cusp, acting as a constraint, on the resonance parameters determined in the fit is emphasized. The fit also determines the phase of the ηN production amplitude at the ηn threshold, which then using the knowledge of the orientation of the cusp gives information on the phase of the elastic no-spin-flip amplitude at the ηn threshold. This information could be a useful constraint in πN partial-wave analysis.

Just above the ηN threshold (1488 MeV), the πN S_{11} amplitude has a prominent N' resonance which has a large branching ratio (~65%) for the ηN channel. As a result, η production is large, and the $(\pi N \to \eta N)$ cross section, which varies linearly with the ηN center-of-mass momentum near the ηN threshold, increases very rapidly with the pion laboratory momentum. This rapid rise in the production cross section manifests itself as a sharp cusp at the ηN threshold in the πN elastic differential cross section.

Recently Debenham *et al.*[1] have reported measurements of the differential cross section for the reactions $\pi^- p \to \pi^- p, \pi^0 n, \eta n$ in the near-backward direction. The data for the reaction $\pi^- p \to \pi^- p$ clearly shows a cusplike structure at the ηn threshold. Consequently, an analysis of the data around the ηn threshold reveals via the unitarity relation the size and the orientation of the cusp; more specifically, the production slope or the rate of the reaction $(\pi^- p \to \eta n)$ as measured with respect to the ηn center-of-mass momentum, and the phase of the ηN production amplitude relative to half the phase of the backward πN elastic amplitude are determined at the ηn threshold. Further, by a comparison of the above phase relationship with the phase of the backward πN elastic amplitude as calculated from the amplitudes of the Saclay partial-wave analysis,[2] the phase of the production amplitude at the ηn threshold is estimated. This is then used as a constraint in conjunction with the production slope, in fitting the elastic πN S_{11} amplitude through the ηn threshold and the resonance, lying above it. The parameters of the resonance, extracted from the fit, show significant dependence on the aforementioned constraints. The fit also fixes more accurately the phase of the production amplitude, which together with its phase relationship with the backward πN elastic amplitude, yields information on the πN elastic amplitude at the ηn threshold.

The $\pi^- p$ elastic differential cross section is expressed in terms of the well-known no-spin-flip and spin-flip amplitudes, f and g, as

$$\frac{d\sigma}{d\Omega} = |f|^2 + |g|^2 . \tag{1}$$

In either the backward or the forward direction, g vanishes, since in either case there is no spin flip. Further, the elastic S_{11} amplitude makes a contribution only to f in the following simple way:

$$f = \tfrac{2}{3} t + \text{other partial-wave amplitudes} , \tag{2}$$

where the factor $\frac{2}{3}$ is due to the isospin coefficients and t is defined as

$$t = \frac{\eta e^{2i\delta} - 1}{2iq} , \tag{3}$$

q being the $\pi^- p$ center-of-mass momentum. The partial-wave amplitude t has a square-root cut (in the invariant variable s, the center-of-mass energy squared) at the ηn threshold. It is the reflection of this threshold behavior in the differential cross section that we want to study here. The contribution of t to the differential cross section can easily be extracted if we separate out explicitly the square-root cut term in t. In other words, if we write

$$t = t^0 + i t' q_\eta + O(q_\eta^2) , \tag{4}$$

where q_η is the ηn center-of-mass momentum and t^0 the threshold value of t, then using Eqs. (1), (2), and (4), we have in the neighborhood of the

ηm threshold

$$\frac{d\sigma}{d\Omega} = |f^0|^2 + |g^0|^2 + \tfrac{4}{3}\,\mathrm{Re}(if^{0*}t'q_\eta) + O(q_\eta^2)$$

$$= |f^0|^2 + |g^0|^2 - \tfrac{4}{3}\,\mathrm{Im}(f^{0*}t')\,|q_\eta| + O(q_\eta^2) \quad \text{for } q_\eta^2 > 0 \tag{5a}$$

$$= |f^0|^2 + |g^0|^2 - \tfrac{4}{3}\,\mathrm{Re}(f^{0*}t')\,|q_\eta| + O(q_\eta^2) \quad \text{for } q_\eta^2 < 0\,, \tag{5b}$$

where the superscript zero refers to the ηm threshold. In Fig. 1, we show how the data of Ref. 1 look when plotted against the variable $q_\eta^2/|q_\eta|$. The cusplike structure at the ηm threshold is presumably due to the square-root terms in Eqs. (5a) and (5b). It is now clear that a determination of the coefficients of the $|q_\eta|$ term alone, above and below the threshold, gives the relative phase between f^0 and t'. Since g^0 vanishes in the backward direction, one can, further, by determining the constant term, namely $|f^0|^2$, deduce the magnitude of t'. We now show in the following that t' is just the square of the $(\pi N \to \eta N)$ S_{11} amplitude at the ηm threshold.

For a partial wave of angular momentum l, the T matrix for coupled channels can be written[3] as

$$T = \frac{1}{Q^{-1}MQ^{-1} - iQ}\,, \tag{6}$$

where Q is a diagonal matrix of center-of-mass momenta of the coupled channels. The matrix M is symmetric and real, and thus, does not have direct-channel unitarity cuts. For s waves, $l=0$ and T is simply $1/(M-iQ)$. We take T to be a 3×3 matrix because we have effectively three channels, namely, the πN, the ηm, and a third channel to account for all other inelastic processes, which, incidentally, are inappreciable in this problem. Consequently, we write

$$T = \begin{bmatrix} t & r \\ r^T & u \end{bmatrix}, \quad M = \begin{bmatrix} m & d \\ d^T & c \end{bmatrix}, \quad Q = \begin{bmatrix} q & 0 \\ 0 & q_\eta \end{bmatrix}, \tag{7}$$

where t, m, and q are 2×2 matrices that involve the $\pi^- p$ and the third channel; the ηm channel, thus, occupies the third row and the third column; r is a 2×1 column vector, the first element of which is the $(\pi N \to \eta N)$ S_{11} amplitude. The corresponding column vector in M is d. u and c are mere numbers. q is diagonal in the center-of-mass momenta of $\pi^- p$ and the third channel. [Note that the elastic S_{11} amplitude and the $\pi^- p$ center-of-mass momentum, which appeared as t and q, respectively, in Eq. (3), are now given by the first diagonal elements of the t and q matrices, and are thus denoted by t_{11} and q_1, respectively, hereafter.]

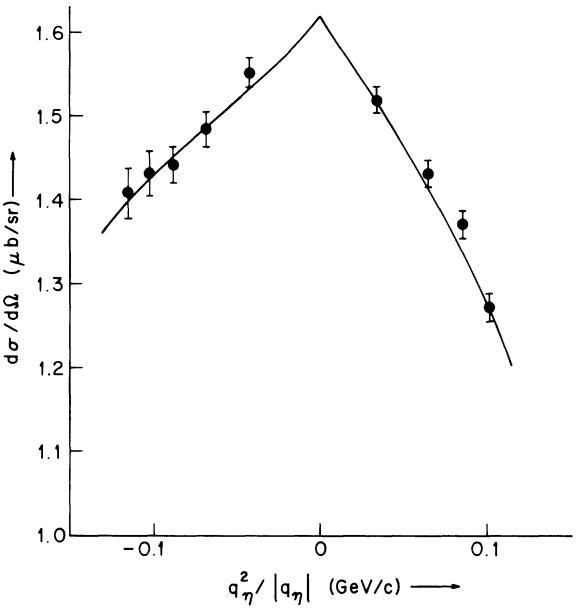

FIG. 1. $\pi^- p$ elastic backward differential cross-section data at $\cos\theta = -0.9952$ plotted against the ηn center-of-mass momentum. Data are taken from Ref. 1. The normalization uncertainties are not included. The curve is our fit to the above data.

Now from Eq. (6), it is easy to show that

$$r = -td/c(1 + iq_\eta/c)\,, \tag{8a}$$

$$t = [(m - iq) - dd^T/c - iq_\eta dd^T/c^2]^{-1}\,. \tag{8b}$$

Then, at threshold, where $q_\eta = 0$, we have

$$r^0 = -t^0 d/c \tag{9a}$$

and

$$t^0 = [(m - iq) - dd^T/c]^{-1}\,. \tag{9b}$$

Note that the q matrix is essentially constant near the threshold. Substitution of Eqs. (9a) and (9b) in Eqs. (8a) and (8b) yields

$$t = t^0 + iq_\eta r^0 r^{0T}\,. \tag{10}$$

The elastic S_{11} amplitude from Eq. (10) is

$$t_{11} = t_{11}^0 + iq_\eta (r_1^0)^2\,. \tag{11}$$

Comparing Eq. (11) with Eq. (4), we find that

$$t' = (r_1^0)^2\,, \tag{12}$$

the square of the $(\pi N \to \eta N)$ S_{11} amplitude at the ηm threshold; the phase of t' is simply twice that of r_1^0. If we look at the expression for the production cross section,

$$\sigma(\pi^- p \to \eta n) = (\tfrac{2}{3})4\pi q_\eta/q_1\,|r_1^0|^2 \tag{13}$$

(the factor $\frac{2}{3}$ is from the isospin coefficients), we see that the square of the magnitude of r_1^0 determines the slope of the production cross section with respect to the ηn center-of-mass momentum, or vice versa.

For the analysis of the cusp, the input data we used are the following:

(1) We used the near backward $\pi^- p$ differential cross section from Ref. 1 at $\cos\theta = -0.9952$, -0.9857, -0.9691 and at pion laboratory momenta (in MeV/c) 656.0, 662.6, 669.3, 676.0, 682.8, 689.7, 696.7, 703.7, and 710.8. (We properly take into account the normalization uncertainties which are about 7% and uncorrelated among the three angles but correlated over a range of fifteen consecutive momenta. There is a 0.1% systematic uncertainty in the momentum determination, which is also included in our analysis.)

(2) We also used the backward differential cross section reconstructed from the results of Saclay partial-wave analysis[2] at pion laboratory momenta (in MeV/c) 657.3, 675.0, 705.8, and 725.4.

(3) In addition, we used the slope (b) of the ηn production cross section versus the ηn center-of-mass momentum: $b = 21.2 \pm 1.8$ mb/(GeV/c), as reported in Ref. 4. In using Eqs. (5a) and (5b) to fit the data, we allowed additional q_η^2 and q_η^4 terms for the background. We also tried to parametrize any angular variations; however, they turned out to be negligible. The values constructed from the Saclay phase shifts do not cover the threshold neighborhood adequately enough to show the cusp structure. The relative phase between t' and f^0 is essentially determined by the data of Ref. 1. The Saclay values, nevertheless, help in the fixing of the normalization of the data of Ref. 1. The result of our calculation is

$$\arg(r_1^0) - \tfrac{1}{2}\arg(f^0) = 26^\circ \pm 6^\circ . \qquad (14)$$

The slope of b of the ηn production cross section is not well determined from the differential cross-section data alone, but the value we get [$b = 24.7 \pm 6.9$ mb/(GeV/c)] is consistent with the direct measurement of Ref. 4. Thus for the fitting of the S_{11} partial-wave amplitude, whose features we describe below, we used instead of our value of b the value of Ref. 4. The other constraint, namely, the phase of the production amplitude, is deduced from Eq. (14), using the value of $\arg(f^0)$, as given by the Saclay partial-wave amplitudes. The value we get is $41^\circ \pm 6^\circ$.

Writing

$$S_E = S_R S_B , \qquad (15)$$

where S_E is the S-matrix element for the elastic channel, and S_R, S_B are those corresponding to the

TABLE I. Results of the fit to the S_{11} amplitude, which resonates in the 1550-MeV region. We used the following constraints: (i) $b = \sigma(\pi^- p \to \eta n)/q_\eta = 21.2 \pm 1.8$ mb/(GeV/c); (ii) $\arg(r_1^0) = \arg(T^0_{\pi^- p \to \eta n}) = 41^\circ \pm 6^\circ$.

No.	Type of fit	χ^2/D.F.	Slope, b [mb/(GeV/c)]	$\arg(r_1^0)$	Mass (MeV)	Width (MeV)	Elasticity	Pole (MeV) Real	Pole (MeV) Imag.	Residue (MeV) Real	Residue (MeV) Imag.	a_1	a_2
1	Without constraints	2.00	15.1 ± 3.7	42.6° ± 6.9°	1543 ± 7	118 ± 48	0.298 ± 0.029	1523 ± 6	−59 ± 17	17 ± 21	13 ± 8	0.062 ± 0.014	0.36 ± 0.13
2	With constraints	1.90	20.6 ± 1.8	39.3° ± 4.7°	1547 ± 6	139 ± 33	0.297 ± 0.026	1519 ± 4	−70 ± 16	20 ± 21	13 ± 8	0.067 ± 0.004	0.48 ± 0.04

resonant and background parts, respectively,

$$T_E = S_B T_R + T_B . \tag{16}$$

T_R is the resonant amplitude, parametrized as

$$T_R = \frac{a_1\phi_1}{s_0 - s - ia_1\phi_1 - ia_2\phi_2 - ia_3\phi_3 - ia_4\phi_4} , \tag{17}$$

where ϕ_1 and ϕ_2 are the phase-space factors for the πN and the ηN channel, respectively, behaving like the center-of-mass momentum near their respective thresholds, while ϕ_3 and ϕ_4 are the phase-space factors for the $\pi\pi N$ and the $\pi\Delta$ channels assumed also to be coupled to the resonance. The above parametrization for T_R and that used for T_B are identical with those of Cutkosky *et al.*[5] Note also that the amplitudes are parametrized to conform to the definition $S = 1 + 2iT$. For the fit, the Saclay partial-wave amplitudes are used in an approximate range of 1350–1550 MeV. Below 1350 MeV and extending almost to the elastic threshold, the data points are those of Carter *et al.*,[6] while above 1550 MeV and up to 1650 MeV,[7] the points are from the LBL-CMU collaboration.[5]

Table I shows the results of the fit with and without the use of constraints. The high value of χ^2 per degree of freedom is ascribable partly to the somewhat erratic nature of the data of Carter *et al.* and partly to the fact that the errors on the data points of Carter *et al.* and Saclay analysis are underestimated. The parameters shown in the table and the errors on them were calculated, as mentioned in Ref. 5. It is clear from a comparison of the two fits that the use of constraints enables a more accurate determination of the parameters. The changes caused in the values of the parameters are understood roughly as follows: The contribution of the background amplitude to the slope is observed to be negligible, i.e., the parametrized form of slope is resonant in character. Consequently, the slope constraint causes a_2 to increase. To compensate for this, a_1 tends to increase, but is checked somewhat by the phase constraint, namely $\arg(r_1^0)$, since it depends quite sensitively on a_1 in its parametrized form. The width and the imaginary part of the pole, therefore, register an increase. An interesting feature of the fit is an appreciable difference in the mass of the resonance and the real part of the pole. To understand this, one observes that the pole position is given essentially by

$$(E_0 - E - i\gamma_1\phi_1(E) - i\gamma_2(E - E_T)^{1/2})\big|_{E=E_P=R_P-iI_P} = 0 , \tag{18}$$

where E_0, E are the energies corresponding to the invariant variables s_0, s in the denominator of T_R,

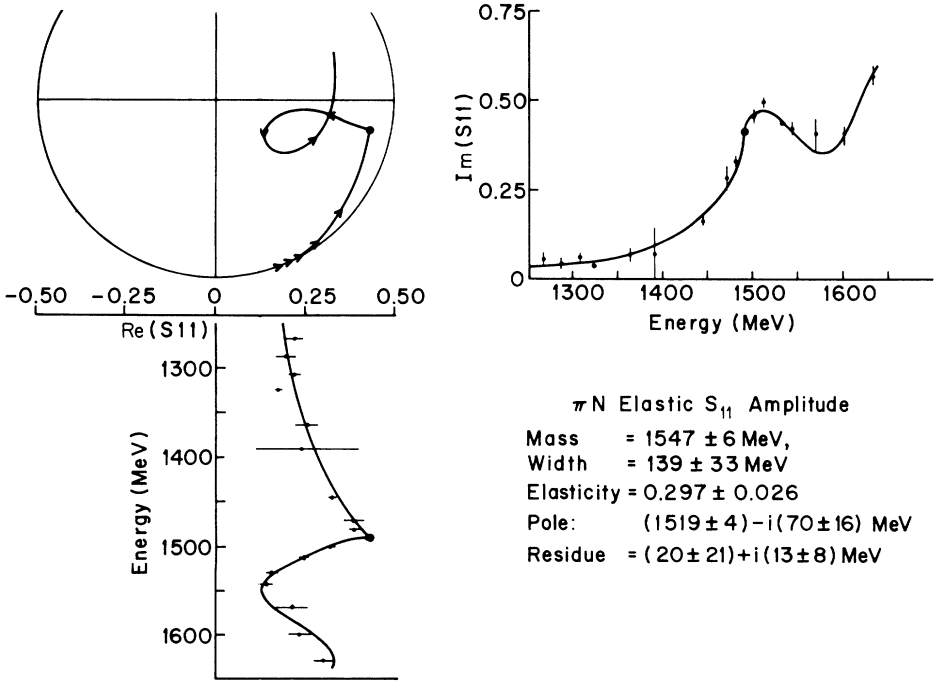

FIG. 2. $\pi N S_{11}$ amplitude which resonates above the ηN threshold in the 1550 MeV region. The fitted real and imaginary parts, plotted against center-of-mass energy, are shown as continuous lines. On the Argand plot, points at intervals of 50 MeV, starting from 1250 MeV, are indicated by arrows. The dot on the plots is the point corresponding to the ηn threshold.

E_T the ηN threshold energy, and E_P the pole position; terms involving a_3 and a_4 are absent because of their insignificant coupling to the resonance, and γ_1 and γ_2 are proportional to a_1 and a_2. Then, under the assumption of $I_P \gg (R_P - E_T)$ (which approximately holds) and $\phi_1(E_P)$ being almost real, and working up to first order in $(R_P - E_T)/I_P$, one finds from Eq. (18) that

$$E_0 - R_P = \gamma_2 \left(\frac{I_P}{2}\right)^{1/2} \left(1 - \frac{R_P - E_T}{2I_P}\right), \tag{19}$$

which clearly depends strongly on the coupling of the ηN channel to the resonance. It is worthwhile mentioning that, under similar circumstances but with the resonance lying below the threshold of the channel to which it is strongly coupled, $E_0 < R_P$. I_P, on the other hand, is very nearly equal to half the width $\Gamma_0/2$. Explicitly, up to first order in $(R_P - E_T)/I_P$,

$$\frac{\Gamma_0}{2} - I_P = \gamma_2 \left[(E_0 - E_T)^{1/2} - \left(\frac{I_P}{2}\right)^{1/2} \left(1 + \frac{R_P - E_T}{2I_P}\right)\right], \tag{20}$$

which is negligibly small. Figure 2 shows the fit and the Argand plot of the S_{11} amplitude. In the latter there is a right-angle turn, as expected. The phase of the elastic S_{11} amplitude at this energy is 44°, which is close to the value $39.3° \pm 4.7°$ for $\arg(r_1^0)$, in agreement with the requirements of unitarity.

In short, the fit we have obtained has the feature of incorporating whatever information we have on the behavior of this amplitude near the ηn threshold. The resonance parameters thus obtained may be regarded as more reliable and could be used to test the predictions of symmetry models on the partial widths of this resonance for the πN and the ηN channels. Further, from Eq. (14) we find, using the fitted value of $\arg(r_1^0)$, that $\arg(f^0) = 26° \pm 12°$. It is interesting to note that with the availability of data on πN differential cross-section data at other angles near the ηN threshold, similar cusp analyses could yield information on the angular variation of the elastic no-spin-flip amplitude, f^0. This information could be of considerable use in further work on partial wave-analyses.

We thank Professor R. E. Cutkosky for very helpful suggestions and discussions. We are also indebted to authors of Ref. 5 for allowing us use of some of their computer programs.

---

*Work supported in part by the Energy Research and Development Administration.

†Present address: Division of Nuclear Science and Engineering, Carnegie-Mellon University, Pittsburgh, Pennsylvania 15213.

[1]N. C. Debenham *et al.*, Phys. Rev. D 12, 2545 (1975).

[2]R. Ayed and P. Bareyre, private communication to the Particle Data Group.

[3]See, e.g., M. Ross and G. Shaw, Ann. Phys. (N.Y.) 13, 147 (1961).

[4]D. M. Binnie *et al.*, Phys. Rev. D 8, 2789 (1973).

[5]R. E. Cutkosky *et al.*, Phys. Rev. Lett. 37, 645 (1976).

[6]J. R. Carter *et al.*, Nucl. Phys. B58, 378 (1973).

[7]A second resonance actually occurs in this region; we, therefore, include it as a part of background.